ACS OMEGA

http://pubs.acs.org/journal/acsodf

Article

Effect of Co-combustion of Multiple Additives with Coal on NO Removal

Shuqin Wang,* Hao Fu, Lifeng Liu, ZhiQiang Zhang, Mingzhu Liu, and Ying Huang

Cite This: *ACS Omega* 2021, 6, 33676−33684

Read Online

ACCESS | Metrics & More | Article Recommendations

ABSTRACT: Denitrification experiments of co-combustion of coal and additives were carried out in a horizontal tube furnace. The results showed that calcium acetate limited the production of NO_2. The optimum calcination temperature of CTAB-Zr-TiO_2 was 673 K. The denitrification efficiency reached up to 72.27%, and desulfurization efficiency reached 83.03% when corncob, calcium acetate, and CTAB-Zr-TiO_2 were added. Corncob, calcium acetate, and CTAB-Zr-TiO_2 all promoted coal combustion. The specific surface area of CTAB-Zr-TiO_2 (55.50 m^2/g) was the largest, which was more than 4.5 times that of pure TiO_2 (12.20 m^2/g). The denitrification process in the co-combustion of coal with multiple additives included a homogeneous reaction and heterogeneous reaction. The homogeneous reaction was that NO and NO_2 were reduced to N_2 by reducing gases produced in combustion. The heterogeneous reaction involved the reduction of NO and NO_2 by coal char. The additives increased the specific surface area of the coal char and enhanced the activity of the heterogeneous reduction of NO and NO_2. At the same time, the catalysis of alkali metal oxides in corncob and CTAB-Zr-TiO_2 promoted the heterogeneous reduction of NO and NO_2 by the coal char.

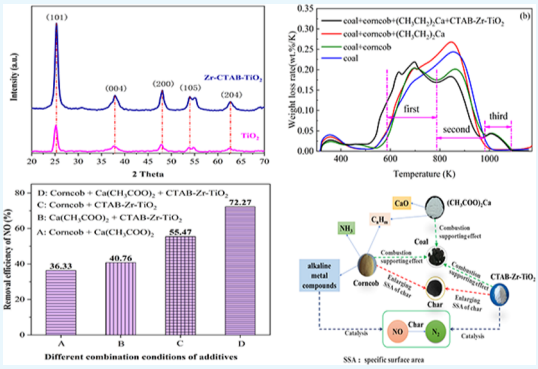

1. INTRODUCTION

Energy is produced through the combustion of coal, and nitrogen oxides (NO*x*) are the main air pollutants produced in the process.[1] Currently, the main technologies for reducing NO*x* emissions are flue gas denitrification and low-NO*x* combustion technology.[2] The technology and equipment required for low-NO*x* combustion are not yet ready for comprehensive application. The main reduction methods used in coal-fired power plants are the SCR method and SNCR method,[3−5] and only SNCR is suitable for high temperature. However, SNCR requires a large amount of reductant, and the treated nitrogen oxide still faces difficulty in meeting the ultra-low emission requirements, so additional processing costs are required.[6] Therefore, an economical and reliable technology must be developed for controlling NO*x* emissions in coal-fired processes. Many studies have indicated that NO*x* emissions can be controlled by adding chemical components such as carbon monoxide, ammonia, unburned hydrocarbons, and limestone.[7,8] Using small amounts of chemical additives to limit NO*x* emissions is simple, highly efficient, and inexpensive.[9]

The desirability of new pollutant-treatment technologies based on clean energy sources has increased due to the serious environmental changes caused by the production of non-renewable energy. Some studies have indicated that the co-combustion of coal and biomass can increase the ignition point, enhance the ignition performance, and facilitate the complete combustion of coal in the furnace because of the low ignition temperature and abundant volatile content of biomass.[10,11] In addition, the emission concentration of sulfur oxide (SO*x*), NO*x*, and other pollutant emissions is lower when coal is co-combusted with biomass.[12,13] Zhang et al. found that the peanut shell reburned at 800 °C with a denitrification efficiency of 41.58% and desulfurization efficiency of 10.25%.[14] Liu et al.[15] found a synergistic effect of bituminous coal with corncob or hardwood. Moreover, they found that the combustion of a mixture of biomass and coal outperforms that of coal alone. However, the abundant alkali metals (e.g., potassium and sodium) and chlorine in biomass can easily cause slagging in fluidized bed combustion.[16]

Calcium-based additives are effective flue-gas desulfurization agents.[17] Studies have shown that organic calcium compounds (OCCs) decompose easily and produce numerous hydrocarbons (C_mH_n) at high temperature. These hydrocarbons can reduce NO. The CaO produced by OCCs at high temperatures catalyzes the heterogeneous reduction of NO by coal

Received: August 26, 2021
Accepted: November 23, 2021
Published: December 4, 2021

Table 1. Proximate and Ultimate Analysis Results for Coal and Biomass (wt %, Air-Dry Basis)

samples	proximate analysis				ultimate analysis				
	moisture	ash	volatiles	fixed carbon	carbon	hydrogen	oxygen	nitrogen	sulfur
coal	3.14	18.29	27.60	50.97	56.69	3.86	14.81	1.04	2.17
corncob	3.78	0.02	76.00	20.20	44.43	6.25	44.82	0.62	0.08

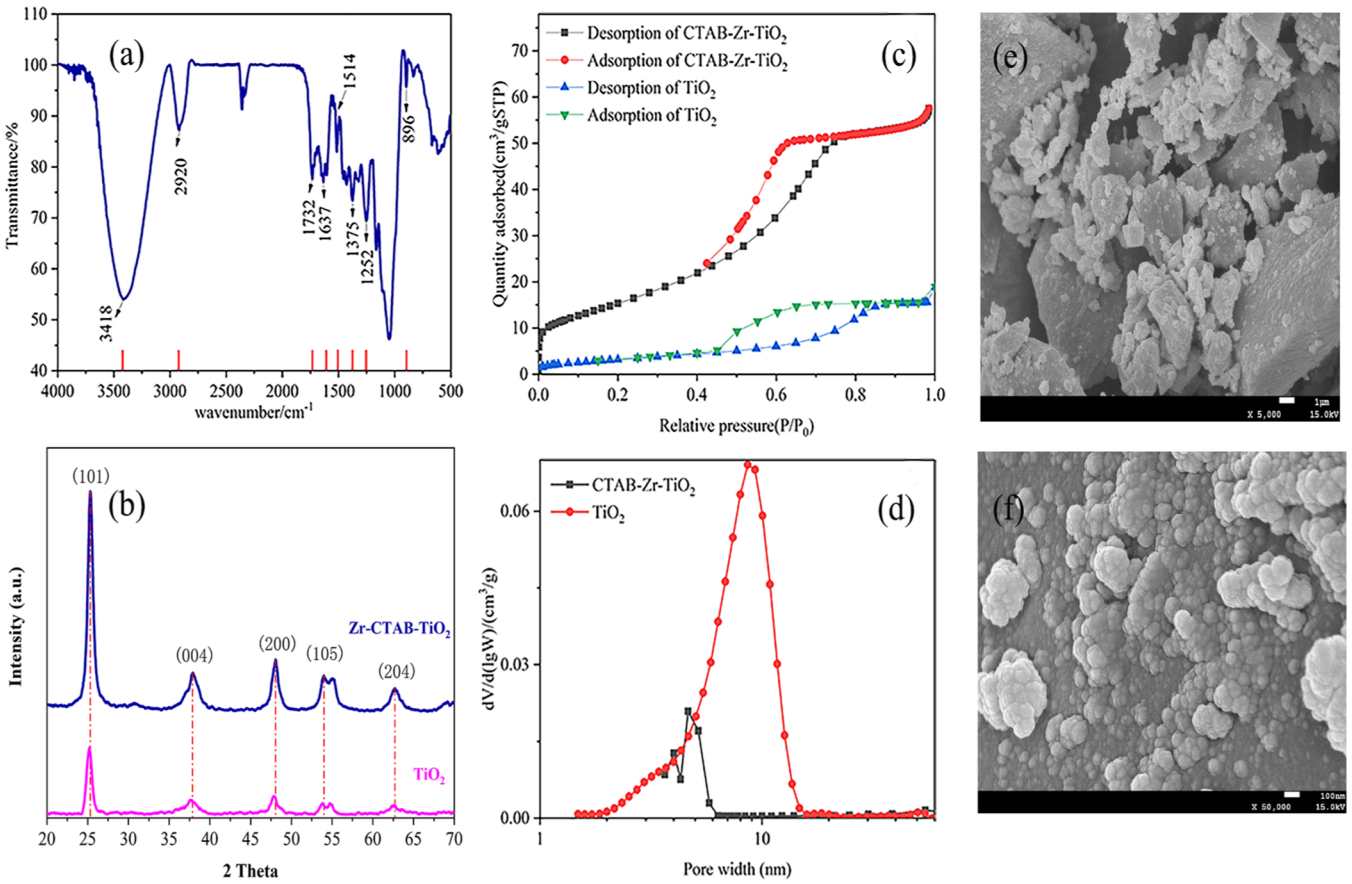

Figure 1. (a) FT-IR spectra of corncob, (b) XRD patterns of TiO_2 and CTAB-Zr-TiO_2, (c,d) N_2 adsorption isotherm (c) and pore distributions (d) of pure TiO_2 and CTAB-Zr-TiO_2, and (e,f) SEM images of CTAB-Zr-TiO_2 (e) ×5000, (f) ×50 000.

char; thus, the production of CaO reduces the NO released.[14,18] Consequently, the addition of OCCs and biomass in coal combustion reduces the slagging in biomass and coal combustion and the NO*x* emitted in flue gas.

Daood et al.[19] proposed that additives (such as SiO_2, TiO_2, and Fe_2O_3) added in small quantities to the co-combustion of coal and biomass can enhance the decomposition of volatile hydrocarbons to promote the reduction of NO and reduce NO*x* emissions. Because of the small specific surface area of pure TiO_2, its catalytic activity is limited. Some studies have indicated that doping a few transition metal ions (such as Mn, Ce, etc.) into TiO_2 can inhibit lattice growth, increase the specific surface area, and improve catalytic efficiency.[20] These studies have shown that the addition of a rare earth element can significantly enhance the activity of the catalyst. In addition, the doping of Zr at low temperature has been studied,[21−23] but there are few studies at high temperature. Therefore, Zr was doped into TiO_2 as a doping element in this paper. The pore volume, specific surface area, and adsorption capacity of TiO_2 can be increased by adding a pore-forming agent. Yi et al.[24] used ultrasonically assisted pore-forming agents [cetyltrimethylammonium bromide (CTAB), NH_4NO_3, and urea] to modify the surface of the adsorbent Al_2O_3@TiO_2−Ce. In their study, the CTAB-modified adsorbent exhibited the most effective denitrification. Therefore, CTAB was used in this study as a pore-forming agent in the preparation of TiO_2.

In recent years, we found that adding multiple additives in the process of coal combustion can promote the removal of NO*x*, SO_2, Hg, and other pollutants.[25−27] The results showed that the modified TiO_2 increased combustion efficiency, promoted calcium oxide desulfurization, and effectively alleviated the slagging problem of the boiler caused by desulfurizers and biomass.[25,26] We found that multiple additives effectively improved the efficiency of mercury removal and desulfurization, but the denitrification efficiency was only about 43%.[27] Therefore, to improve the efficiency of denitrification, this paper continued to study the effects of various additives such as biomass corncob, desulfurizer, and modified TiO_2 on the denitrification and denitrification mechanism during coal combustion. This study provides theoretical guidance for the resource utilization of biomass and the feasibility of co-combustion technology in the circulating

https://doi.org/10.1021/acsomega.1c04675
ACS Omega 2021, 6, 33676−33684

fluidized bed, decreases the use of the reductant, and reduces the cost of the subsequent treatment of the flue gas.

2. RESULTS AND DISCUSSION

2.1. Characterizations of Samples. Table 1 presents the results for the ultimate and proximate analyses of coal and corncob. Table 1 indicates that the nitrogen content of the coal (fuel-N of 1.04%) was higher than that of the biomass (fuel-N of 0.62%). In addition, the volatile-matter content of coal (27.60%) was lower than that of corncob (76.00%). Plenty of volatile matter in the biomass precipitated rapidly at a reaction temperature of 1123 K. Consequently, an oxygen-inadequate zone formed in the local combustion area of the coal, promoting conversion of HCN to N_2 and reducing the generation of NO.

Figure 1a displays the Fourier-transform infrared spectra of corncob. The peaks at 3418, 1375, and 896 cm^{-1} corresponded to the stretching vibrations of the hydroxyl group. The peaks at 1732, 1637, 1514, and 1252 cm^{-1} corresponded to the stretching vibrations of the C═O group. Thus, corncob contained carboxyl groups. The peaks at 2920 cm^{-1} can be assigned to aromatic CH_3 group stretching. Under combustion in the oxygen atmosphere, the carboxyl, C═O, and aromatic CH_3 groups in the cellulose, hemicellulose, and lignin of corncob were easily oxidized to CO_2 and H_2O, which competed with nitrogen in coal for oxygen and inhibited nitrogen oxidation to NO.

The crystal structures of the CTAB-Zr-TiO_2 and pure TiO_2 catalysts were analyzed using XRD patterns. Figure 1b displays the wide-angle XRD patterns of various catalysts. Compared with pure TiO_2, no additional diffraction peak was observed for CTAB-Zr-TiO_2. Characteristic peaks corresponding to the (101), (004), (200), (105), and (204) planes were observed for anatase TiO_2. These characteristic peaks for CTAB-Zr-TiO_2 were shifted slightly to the right, and the characteristic peaks of anatase became higher and narrower. The results indicated that the modifiers changed the octahedral structure of TiO_2 and distorted its lattice. Lattice distortion increased the oxygen vacancies on the catalyst surface, thereby enabling adsorption of additional oxygen atoms.

Through the line−width analysis of the (101) diffraction peak of anatase, the average crystal sizes of CTAB-Zr-TiO_2 and pure TiO_2 were estimated to be 9.80 and 10.24 nm, respectively, by using the Scherrer equation. The crystal size of TiO_2 decreased with CTAB and Zr doping, indicating that CTAB and Zr doping inhibited grain growth. Furthermore, during synthesis, the insertion of CTAB and Zr into the TiO_2 matrix hindered the agglomeration and crystallization of TiO_2 crystals, reducing the crystal size. The smaller the grain is, the larger is the specific surface area.

The surface area and pore structure of catalysts were investigated through N_2 adsorption−desorption measurement. As displayed in Figure 1c, all the catalysts exhibited a reversible type IV isotherm, which is a vital characteristic of mesoporous materials. Both CTAB-Zr-TiO_2 and TiO_2 catalysts exhibited the H1 hysteresis loop, which indicated the ordered mesoporous structure. Figure 1d indicates that the CTAB-Zr-TiO_2 and TiO_2 catalysts exhibited the concentrated pore size in the range of mesopores. The most probable common radius of pure TiO_2 and CTAB-Zr-TiO_2 was 8.63 and 4.65 nm, respectively.

Table 2 presents the pore volume, pore size, and specific surface area per the BET model for various catalysts. The specific surface area of CTAB-Zr-TiO_2 (55.50 m^2/g) was more than 4.5 times that of pure TiO_2 (12.20 m^2/g). The pore volume of pure TiO_2 was 0.02 m^3/g and that of CTAB-Zr-TiO_2 was increased to 0.09 m^3/g. However, the pore size of pure TiO_2 was 7.91 nm and that of CTAB-Zr-TiO_2 was reduced to 3.15 nm. The results were consistent with the XRD results. Therefore, CTAB and Zr doping promoted TiO_2 grain dispersion.

Table 2. Pore Volume, Pore Width, and Specific Surface Area of Different Catalysts

samples	$S_{BET}/(m^2 \cdot g^{-1})$	$r_P/(nm)$	$V_P/(cm^3 \cdot g^{-1})$
TiO_2	12.20	7.91	0.02
CTAB-Zr−TiO_2	55.50	3.15	0.09

Figure 1e depicts the SEM images of the CTAB-Zr-TiO_2 sample. CTAB-Zr-TiO_2 exhibited irregular morphologies with abundant piled pores of various shapes and sizes. Consequently, the catalyst had a large specific surface area. Moreover, as depicted in Figure 1f, the catalyst surface exhibited a bulge with numerous uneven spherical morphologies. These spherical morphologies comprised micropores, which are crucial for catalysis.

The XRD, SEM, and BET analysis results indicated that CTAB and Zr doping augmented the specific surface area and enhanced the pore structure of TiO_2. In general, it is conducive to catalytic performance after modification.

To study the thermal stability of the samples and the possible effect of additives on the coal combustion process, TG was conducted for ① coal, ② coal + corncob, ③ coal + corncob + calcium acetate, and ④ coal + corncob + calcium acetate + CTAB-Zr-TiO_2. Figure 2 indicates that the mass loss of coal mainly included moisture loss, volatile matter loss, and fixed carbon combustion. The decomposition of samples ①, ②, ③, and ④ ended at 1007, 1089, 1006, and 1094 K, respectively. The solid residues of the samples totaled 31.22, 26.95, 24.15, and 26.92 wt %, respectively. The additives resulted in lower residual mass than that obtained from pure coal combustion. This result indicated that the additives supported combustion. In the initial stage of combustion, the mass loss of sample ④ was larger than that of pure coal. Moreover, the initial combustion rate increased significantly with the addition of CTAB-Zr-TiO_2, which proved CTAB-Zr-TiO_2 supporting combustion. The residual mass after burnout was higher for sample ④ than for sample ③ because of the high quality of the leftover catalyst from the combustion of sample ④.

As seen from Figure 2b, after corncob was added, a typical double peak appeared.[28,29] The first peak represented the biomass volatilization reaction zone (approximately 670−780 K), and the second peak was related to coal combustion (approximately 820−970 K). The decomposition rate in the first stage of the severe weight-loss region was higher with corncob than with pure coal without corncob. The phenomenon occurred because of the decomposition of hemicellulose and cellulose and the softening and decomposition of the lignin in the biomass.[30,31] However, lignin is highly stable and more difficult to decompose than hemicellulose or cellulose.[32] It is speculated that the third peak at approximately 1000 K is related to the decomposition of lignin. The sample mass decreased, and the combustion rate increased after the addition of calcium acetate to the coal and biomass. Therefore, calcium acetate promotes the co-combustion of coal and biomass. The addition of corncob increased the rate of the

https://doi.org/10.1021/acsomega.1c04675
ACS Omega 2021, 6, 33676−33684

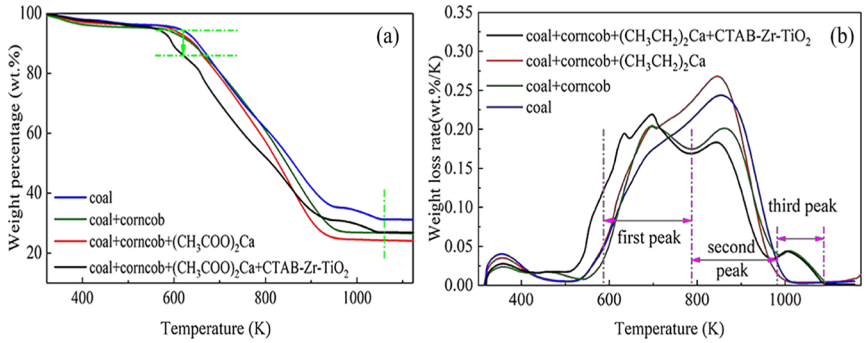

Figure 2. Different mixed coal samples of TG curves (a) and TGA curves (b).

first stage of combustion and decreased the rate of the second stage, making the combustion more stable.

Oladejo et al.[28] found that a synergistic effect occurs when coal is combined with oat straw. Therefore, we speculate that such a synergistic effect may result from the co-combustion of multiple additives with coal. That is, a co-combustion process cannot be considered a simple superposition of multiple combustion processes.

To further explore the denitrification mechanism for the co-combustion of corncob and coal, we analyzed the components of coal ash and coal + corncob ash after combustion. Table 3 lists the main components in the ash. The contents of CaO, MgO, K_2O, Fe_2O_3, and other alkaline oxides were higher in the coal + corncob ash than in the pure coal ash, indicating the abundance of alkaline compounds in corncob. Studies have shown that alkaline substances such as Fe_2O_3 can catalyze NO reduction.[32]

Table 3. Main Components of the Residual Ash Obtained after Combustion (%)

samples	SiO_2	Al_2O_3	Fe_2O_3	CaO	MgO	K_2O	Na_2O
coal	46.62	21.64	12.34	5.38	1.32	0.68	0.58
coal + corncob	38.18	14.68	15.02	8.08	1.81	3.04	0.75

The rate of the temperature increase on the surface of coal and additives was very high when it underwent sudden combustion in the tubular furnace at 1123 K. Thus, the combustion processes of the volatiles and coal char had a common time overlap. In the initial stage of volatilization and combustion, much oxygen was consumed. Moreover, the oxygen content on the coal char surface was almost 0, which was conducive to heterogeneous NO reduction. To clarify the denitrification mechanism of the co-combustion of coal with multiple additives, we conducted an experiment to investigate the removal of NO from the coal char. This experiment was also conducted in the horizontal tubular furnace. First, 0.2 g of coal char was pushed into the furnace at 1123 K. NO gas was subsequently introduced at 40 mL/min, and the reaction time was 15 min. The masses of the coal char and porcelain boat were recorded before and after the reaction. These masses were used to calculate the mass lost during the reaction. The difference in the NO concentration after the addition of the coal char was calculated. The ratio between the difference and the initial NO concentration was considered the denitrification efficiency.

Five types of coal chars were used in the experiment: (a) coal, (b) coal + corncob, (c) coal + corncob + CTAB-Zr-TiO_2, (d) coal + corncob + calcium acetate, and (e) coal + corncob + calcium acetate + CTAB-Zr-TiO_2.

As presented in Table 4, the coal chars exhibited favorable denitrification performance. The denitrification efficiency of all char samples was more than 82%. The sample containing corncob, calcium acetate, and CTAB-Zr-TiO_2 exhibited the highest denitrification efficiency and mass-loss rate and the largest specific surface area. The mass-loss rate of the coal char increased with the denitrification efficiency, suggesting that a chemical reaction occurred during denitrification. The denitrification efficiency of sample b (coal + corncob) was 7.13% higher than that of sample a (coal). A comparison of the denitrification efficiencies of samples c (coal + corncob + CTAB-Zr-TiO_2) and d (coal + corncob + calcium acetate) indicated that CTAB-Zr-TiO_2 and calcium acetate were beneficial for the denitrification reaction of the coal char. Moreover, CTAB-Zr-TiO_2 promoted the combustion of the coal char and augmented the specific surface area. The residual mass of the samples decreased after the addition of the additives in the TG analysis was identified by the results mentioned above.

Table 4. Specific Surface Area, Mass-Loss Rate, and Denitrification Efficiency of Coal Char

samples	specific surface area(m^2/g)	efficiency(%)	mass-loss rate(%)
A	5.52	82	23
B	25.16	89	30
C	55.51	91	49
D	36.20	95	40
E	57.69	97	54

Combined with the above characterization results, it can be speculated as follows: reducing gases were produced during the combustion of corncob and calcium acetate. On the one hand, a large amount of the reducing gas formed the anoxic zone in the local combustion zone, which inhibited the production of HCN, the precursor of NO. On the other hand, the reducing gas reduces NO to N_2 homogeneously. The catalytic action of alkaline metal compounds, such as Fe_2O_3 in corncob, can accelerate the heterogeneous reduction of NO in the coal char; all additives can increase the specific surface area of the coal char, enhance the reactivity of the coal char in heterogeneous reduction of NO, and promote the heterogeneous reduction of NO. To verify this conjecture, the denitrification experiments of co-combustion of coal and additives were carried out.

2.2. Denitrification Experiments. The effect of desulfurizer types on denitrification was investigated. Figure 3 a indicates that the addition of calcium acetate promoted

https://doi.org/10.1021/acsomega.1c04675
ACS Omega 2021, 6, 33676−33684

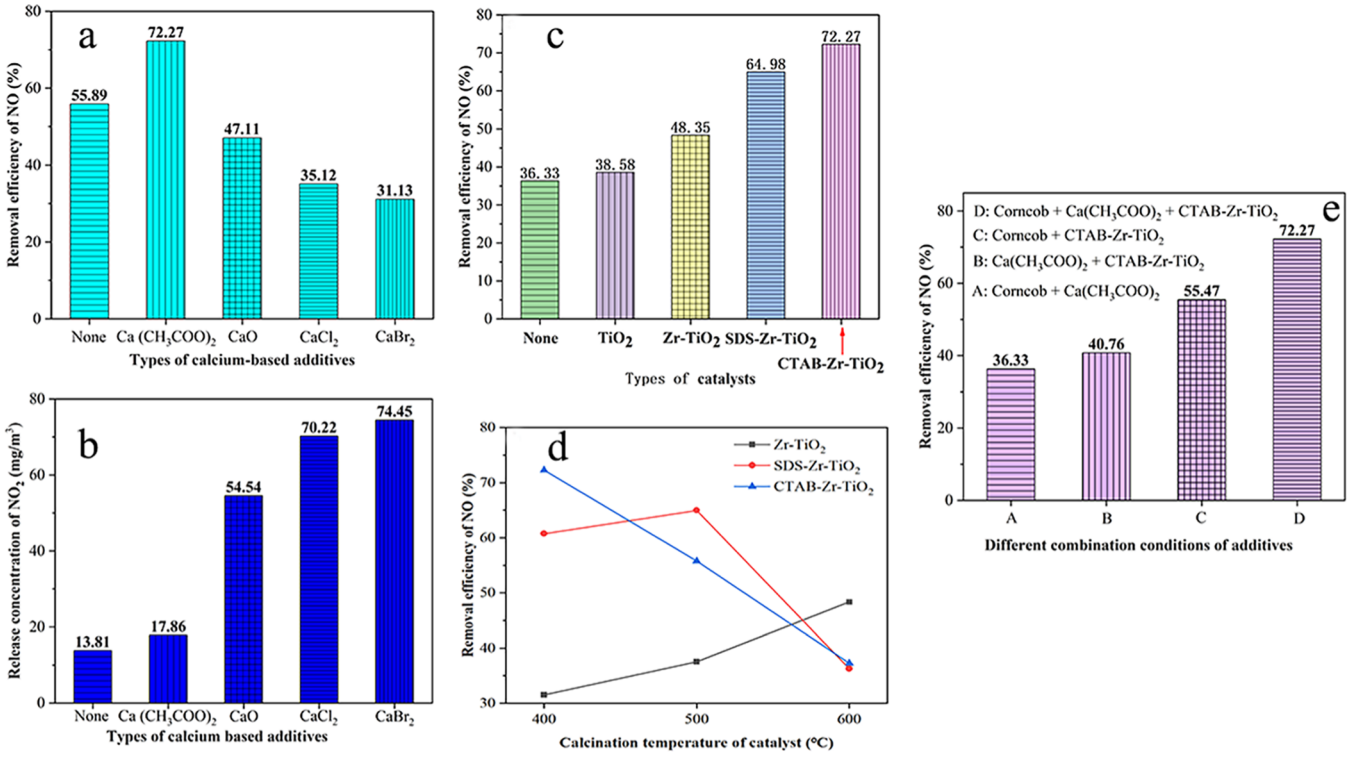

Figure 3. (a) Effect of different calcium-based additives on denitrification efficiency, (b) effect of different calcium-based additives on the release concentration of NO_2, (c,d) effect of different types of catalysts (c) and calcination temperatures (d) on denitrification efficiency, and (e) effect of different combination conditions of additives on denitrification efficiency.

denitrification, whereas the addition of inorganic calcium compounds inhibited denitrification. These findings are consistent with those of Zhang[14] and Niu.[18] Calcium acetate decomposed to form CaO and hydrocarbons (C_nH_m), which reduced some NO to N_2. However, when inorganic calcium compounds were added, the CaO produced by combustion catalyzed the conversion of hydrocarbon nitrogen (HCN) and nitrogen hydrogen (NH_i) compounds to NO and thus reduced the denitrification efficiency.

To further study the influence of the desulfurizer on NO_X emission, the influence of the desulfurizer on NO_2 emission was also studied. Figure 3b indicates that inorganic calcium compounds catalyzed the conversion of HCN and NH_i to NOx and increased NO_2 emissions. This catalytic effect made NO_2 easily reduced by the coal char. The reduction product was mainly NO, and very little N_2 was released. Thus, the addition of CaO not only increased the NO_2 emissions but also decreased NO-removal efficiency.

Therefore, compared with inorganic calcium compounds, calcium acetate is a more suitable denitrification additive. Therefore, calcium acetate was used as a desulfurizer additive in later experiments.

Figure 3c compares the effects of different catalysts on NO-removal efficiency. Figure 3c indicates that the denitrification efficiency was higher with than without a catalyst. The activity of pure TiO_2 was like that of without a catalyst, suggesting that pure TiO_2 was useless for the removal of NO. However, the incorporation of Zr in the TiO_2 framework considerably enhanced the catalytic activity. Moreover, the addition of a pore-forming agent (SDS or CTAB) in Zr-TiO_2 further improved the activity of the catalyst. The order of the catalytic activity was CTAB-Zr-TiO_2 > SDS-Zr-TiO_2 > Zr-TiO_2 > TiO_2. The CTAB-Zr-TiO_2 catalyst exhibited the highest activity, with a NO-removal efficiency of 72.27%, which was approximately 2 times higher than that without a catalyst (36.33%). The results were mainly due to the lattice expansion of TiO_2 caused by Zr^{4+} doping. Moderate lattice expansion increases the oxygen defects, thereby enhancing the catalytic effect of TiO_2. In the preparation of the TiO_2, the pore-forming agents acted as dispersants. Adding a pore-forming agent significantly increased the adsorption capacity, pore volume, and specific surface area of nano-TiO_2; thus, the catalytic performance and denitrification efficiency improved.

Figure 3d indicates that the optimal calcination temperature was different for different modified TiO_2 catalysts. The optimal calcination temperatures of Zr-TiO_2, SDS-Zr-TiO_2, and CTAB-Zr-TiO_2 were 873, 773, and 673 K, respectively. Incomplete growth of catalyst particles and low catalytic activity were observed when the calcination temperature of Zr-TiO_2 was lower than 873 K. When SDS or CTAB was added to the catalyst Zr-TiO_2, the pore-forming agent dispersed well into the catalyst system at low temperatures; thus, the catalytic activity and denitrification efficiency increased. However, at higher temperatures, the framework of the pore-forming agent collapsed, the TiO_2 particles agglomerated, and plenty of grains increased. Thus, the specific surface area of TiO_2 and the denitrification efficiency decreased. Because SDS required a higher volatilization temperature than CTAB, the optimal calcination temperature for SDS-Zr-TiO_2 was higher than that for CTAB-Zr-TiO_2.

The optimal catalyst in this study was CTAB-Zr-TiO_2, which not only exhibited the highest improvement in denitrification efficiency versus pure TiO_2 but also has a low optimal calcination temperature and thus a low energy cost. Therefore, CTAB-Zr-TiO_2 was used in the subsequent experiments.

https://doi.org/10.1021/acsomega.1c04675
ACS Omega 2021, 6, 33676−33684

Scheme 1. Mechanism Diagram of Denitrification by Co-combustion of Multiple Additives and Coal: (a) Effect of Co-combustion of Multiple Additives and Coal on Denitrification and (b) Possible Denitrification Mechanism

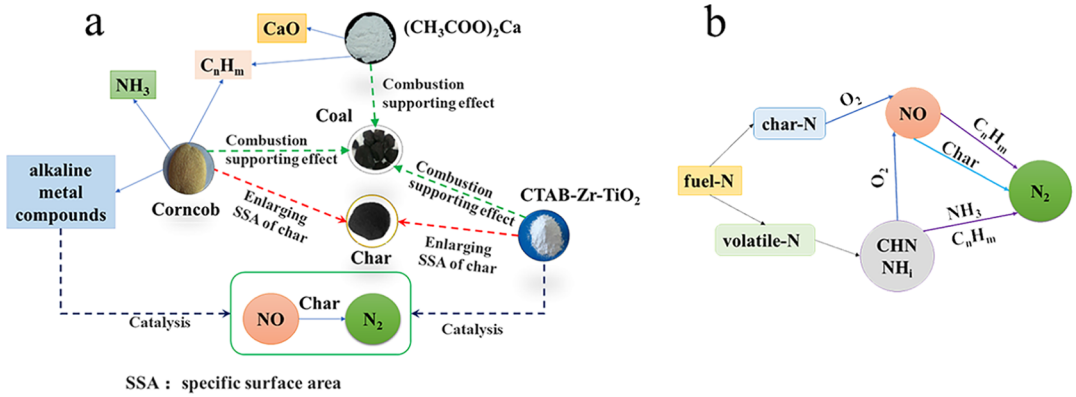

Figure 3e presents the results of NO removal obtained from different combinations of additives. Two additives were used in conditions A, B, and C, and three additives were used in condition D. The denitrification efficiency for condition D was the highest, indicating that the three additives made unique contributions to denitrification. Compared with conditions A, B, and C, the denitrification efficiency of condition D was increased by approximately 17, 32, and 36%, respectively, which indicated that CTAB-Zr-TiO_2 had the greatest effect on denitrification efficiency.

The NO-removal efficiency was 41 and 72% in conditions B [$Ca(CH_3COO)_2$+CTAB-Zr-TiO_2] and D [Corncob + $Ca(CH_3COO)_2$ + CTAB-Zr-TiO_2], respectively. HCN was the dominant volatile-N compound in the combustion of bituminous coal, and it was also the intermediate product of NO production. NH_3 was the dominant volatile-N compound in the combustion of corncob, which enhanced the reduction of NO.[32] Therefore, the addition of corncob improved the denitrification efficiency. The above-mentioned results were consistent with the previous prediction of the effect of additives on the denitrification of co-combustion of coal and additives.

2.3. Denitrification Mechanism for Co-combustion of Multiple Additives with Coal. According to the characterization results of the samples in Section 2.1 and the denitrification experimental results of co-combustion of coal and additives in Section 2.2, the mechanism of denitrification of co-combustion of coal and additives was proposed.

We believe that volatile-N in coal after combustion is oxidized to NO, and a small part of NO is oxidized to NO_2. The denitrification process in the co-combustion of coal with multiple additives (i.e., calcium acetate, corncob, and CTAB-Zr-TiO_2) included a homogeneous reaction and heterogeneous reaction. The homogeneous reaction involved two processes: CnHm and NH_3 were formed during the combustion of calcium acetate and corncob, which easily reduce NO and NO_2 to N_2 and reduce a part of NO_2 to NO. Also, then, plenty of volatile matter separated from corncob resulting in the formation of an oxygen-inadequate zone in coal which inhibited the oxidation of fuel nitrogen and reduced the production of NO and NO_2.

The heterogeneous reaction was the conversion of NO and NO_2 to N_2 by the coal char formed during combustion. The heterogeneous reduction of NO and NO_2 by the coal char was promoted by two approaches. One was that the additives (calcium acetate, corncob, and CTAB-Zr-TiO_2) increased the surface area of the coal char, thus increasing the possibility of the heterogeneous reduction reaction. The other was that the catalysis of alkali metal oxides (such as Fe_3O_4) in biomass and CTAB-Zr-TiO_2 promoted the heterogeneous reduction of NO and NO_2 by the coal char.

The denitrification mechanism for the co-combustion of coal with multiple additives is illustrated in Scheme 1.

3. CONCLUSIONS

Calcium acetate with good desulfurization, TiO_2 with good denitrification performance, and corncob chosen as mixed burning biomass were selected. The desulfurization efficiency of calcium acetate reached 83.03%. The denitrification efficiency was 72.27%, which was higher than the denitrification efficiency (43%) of the previous work (corncob, calcium oxide, and V-TiO_2). The optimum calcination temperature of CTAB-Zr-TiO_2 was 673 K, which was lower than that of Zr-TiO_2 (873 K) and SDS-Zr-TiO_2 (773 K). CTAB and Zr doping augmented the specific surface area and enhanced the pore structure of TiO_2. The specific surface area of CTAB-Zr-TiO_2 (55.50 m^2/g) was more than 4.5 times that of pure TiO_2 (12.20 m^2/g).

Both calcium acetate and CTAB-Zr-TiO_2 support combustion, and the corncob makes the combustion more stable. The denitrification process in the co-combustion of coal with multiple additives included a homogeneous reaction and heterogeneous reaction. The formation of C_nH_m and NH_3 reduced NO and NO_2 to N_2 in the combustion. In the meantime, plenty of volatile matter were separated from corncob resulting in the formation of an oxygen-inadequate zone in coal which inhibited the oxidation of fuel nitrogen and reduced the production of NO and NO_2. The heterogeneous reaction was the heterogeneous reduction of NO and NO_2 to N_2 by the coal char formed during combustion. Additives synergistically increased the surface area of the coal char, thus increasing the possibility of the heterogeneous reduction reaction. The catalysis of alkali metal oxides in biomass identified by the ash analysis and CTAB-Zr-TiO_2 promoted the heterogeneous reduction of NO and NO_2 by the coal char.

Finally, this study probes into the influence of additives on coal combustion, reveals the mechanism of denitrification of various additives in the co-combustion process, and provides guidance for energy saving and emission-reduction technology of a circulating fluidized bed.

https://doi.org/10.1021/acsomega.1c04675
ACS Omega 2021, 6, 33676−33684

Scheme 2. Flow Diagram of the Denitrification Experiment

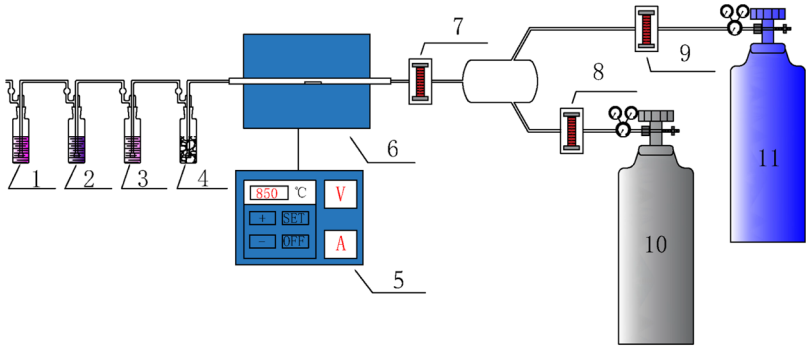

1 absorbent solution	4 cotton	7,8,9 flowmeter
2 $KMnO_4$ solution	5 temperature controller	10 NO
3 absorbent solution	6 resistance furnace	11 O_2

4. MATERIALS AND METHODS

4.1. Materials. All the chemicals were of analytical grade (AR) and used without any further refinement. The following support materials were used: tetrabutyl titanate ($C_{16}H_{36}O_4Ti$; AR, ≥99.0%, Tianjin Kemiou Chemical Reagent), absolute ethanol (C_2H_5OH; AR, ≥99.7%, Tianjin Huihang Chemical Technology), glacial acetic acid [CH_3COOH; AR, ≥99.5%, Fuchen (Tianjin) Chemical Reagent], zirconium oxychloride ($ZrOC_{l2}·8H_2O$; AR, ≥99.0%, Tianjin Kemiou Chemical Reagent), cetyltrimethylammonium bromide (CTAB; AR, ≥99.0%, Shanghai McLean Biochemistry), and sodium dodecyl sulfate (SDS; AR, ≥99.0%, Tianjin Kemiou Chemical Reagent).

4.2. Catalyst Preparation. CTAB-Zr-TiO_2 was prepared by a microwave-assisted sol−gel method. First, 10 mL of absolute ethanol, 40 mL of $C_{16}H_{36}O_4Ti$, and 0.86 g of CTAB were mixed to create solution A. Then, 10 mL of absolute ethanol, 0.38 g of zirconium oxychloride, 3 mL of deionized water, and 2 mL of glacial acetic acid were mixed to create solution B. Subsequently, solution B was slowly added to solution A in a microwave synthesizer at room temperature (298 K) and a power of 200 W. After solution B was added, the temperature was increased to 333 K, and the power was increased to 600 W. The mixture was stirred until a transparent gel was formed. The gel was aged at room temperature (298 K) for 24 h and then dried by a microwave. Finally, the obtained xerogel was calcined in a muffle furnace for 3 h at a set temperature (673, 773, and 873 K), and then, the calcined xerogel was ground into powder to obtain the final catalyst, which was denoted as CTAB-Zr-TiO_2 (CTAB/Ti molar ratio = 2% and Zr/Ti molar ratio = 1%).

The method was also used to prepare Zr-TiO_2, SDS-Zr-TiO_2, and pure TiO_2. However, CTAB was not added to solution A in the preparation of Zr-TiO_2. In SDS-Zr-TiO_2 preparation, SDS (0.68 g, SDS/Ti molar ratio = 2%, Zr/Ti molar ratio = 1%), rather than CTAB, was added to solution A. For pure TiO_2, CTAB was not added to solution A, zirconium oxychloride was not added to solution B, and the xerogel was calcined for 3 h at 773 K in the muffle furnace.

4.3. Coal-Char Preparation. Five types of coal chars were prepared: (a) coal, (b) coal + corncob, (c) coal + corncob + CTAB-Zr-TiO_2, (d) coal + corncob + calcium acetate, and (e) coal + corncob + calcium acetate + CTAB-Zr-TiO_2. The coal samples were placed into capped nickel crucibles. The samples were subsequently heated in the muffle furnace for 10 min at 1123 K without oxygen. Finally, the samples were ground into powder after cooling.

4.4. Experimental Methods. The coal used in the experiment was Shanxi coal, which was produced in the Shanxi province of China. Shanxi coal and corncob were first dried for 2 h at 378 K and then pulverized. The particle size was between 0.075 and 0.095 mm.

The denitrification experiment of co-combustion of coal and additives, which consist of a desulfurizer, catalyst, and biomass, was carried out in a horizontal tube furnace on the premise of ensuring the desulfurization efficiency (the desulfurization efficiency was obtained by the iodine titration method (HJ/T 56-2000) and reached 83.03%). The reaction temperature and pure-oxygen flow rate were set at 1123 K and 40 mL/min, respectively. Then, the fuel (pure Shanxi coal or Shanxi coal with additives) was evenly spread on a small porcelain boat. Finally, the boat was pushed into the middle reaction zone of the ceramic tube of the furnace and burned for 1 h at a constant temperature. The mass of Shanxi coal was 0.5 g, the mass of corncob was 0.33 g (a corncob: Shanxi coal mass ratio of 4:6), and the mass of the catalyst was 0.04 g (the mass of the catalyst was 8% that of Shanxi coal). Calcium acetate chosen as a desulfurizer was added such that the Ca: S molar ratio was 2.3. The flow chart of the experiment is shown in Scheme 2.

The concentration of NO emitted was determined through naphthalene ethylenediamine hydrochloride spectrophotometry (HJ 479-2009). The concentration of NO released during the combustion of Shanxi coal without additives was used as a reference value (C_0). The concentration of NO released during the combustion of mixed coal with additives was denoted as C_1. The removal efficiency η can be calculated using the following formula: $\eta = (C_0 - C_1)/C_0$.

AUTHOR INFORMATION

Corresponding Author

Shuqin Wang − *Department of Environmental Science and Engineering, North China Electric Power University, Baoding 071003, PR China;* orcid.org/0000-0002-9218-8957; Email: wsqhg@163.com

Authors

Hao Fu − *Department of Environmental Science and Engineering, North China Electric Power University, Baoding 071003, PR China*

https://doi.org/10.1021/acsomega.1c04675
ACS Omega 2021, 6, 33676−33684

Lifeng Liu − *Department of Environmental Science and Engineering, North China Electric Power University, Baoding 071003, PR China*
ZhiQiang Zhang − *Department of Environmental Science and Engineering, North China Electric Power University, Baoding 071003, PR China*
Mingzhu Liu − *Department of Environmental Science and Engineering, North China Electric Power University, Baoding 071003, PR China*
Ying Huang − *Department of Environmental Science and Engineering, North China Electric Power University, Baoding 071003, PR China*

Complete contact information is available at: https://pubs.acs.org/10.1021/acsomega.1c04675

Notes

The authors declare no competing financial interest.

■ ACKNOWLEDGMENTS

This work was supported by the National Key Research and Development Plan (grant numbers 2018YFB060420103).

■ REFERENCES

(1) Escudero, A. I.; Aznar, M.; Díez, L. I.; Mayoral, M. C.; Andrés, J. M. From O2/CO2 to O2/H2O Combustion: the Effect of Large Steam Addition on Anthracite Ignition, Burnout and NOx Formation. *Fuel Process. Technol.* **2020**, *206*, 106432.
(2) Liu, X.; Tan, H.; Wang, Y.; Yang, F.; Mikulčić, H.; Vujanović, M.; Duić, N. Low NO combustion and SCR flow field optimization in a low volatile coal fired boiler. *J. Environ. Manage.* **2018**, *220*, 30−35.
(3) Chen, L.; Liao, Y.; Xin, S.; Song, X.; Liu, G.; Ma, X. Simultaneous Removal of NO and Volatile Organic Compounds (VOCs) by Ce/Mo Doping-Modified Selective Catalytic Reduction (SCR) Catalysts in Denitrification Zone of Coal-Fired Flue Gas. *Fuel* **2020**, *262*, 116485.
(4) Cheng, T.; Zheng, C.; Yang, L.; Wu, H.; Fan, H. Effect of Selective Catalytic Reduction Denitrification on Fine Particulate Matter Emission Characteristics. *Fuel* **2019**, *238*, 18−25.
(5) Xu, M.-x.; Wu, Y.-c.; Wu, H.-b.; Ouyang, H.-d.; Lu, Q. Catalytic Oxidation of NH3 over Circulating Ash in the Selective Non-catalytic Reduction Process during Circulating Fluidized Bed Combustion. *Fuel* **2020**, *271*, 117546.
(6) Liu, W.; Wu, B.; Bai, X.; Liu, S.; Liu, X.; Hao, Y.; Liang, W.; Lin, S.; Liu, H.; Luo, L.; et al. Migration and Emission Characteristics of Ammonia/Ammonium through Flue Gas Cleaning Devices in Coal-Fired Power Plants of China. *Environ. Sci. Technol.* **2020**, *54*, 390−399.
(7) Weiqing, Z.; Meng, L.; Baohua, H.; Xiaozhi, Q. Pilot-Scale Study on Improving SNCR Denitrification Efficiency by Using Gas Additives. *Int. J. Chem. React. Eng.* **2019**, *17*, 148.
(8) Liu, H.; Zhao, S.; You, C.; Wang, H. Experimental Study of the Enhancement of the Selective Noncatalytic Reduction Denitrification Process with Methane and Propane in A Circulating Fluidized Bed. *Ind. Eng. Chem. Res.* **2019**, *58*, 7825−7833.
(9) Yao, T.; Duan, Y.; Yang, Z.; Li, Y.; Wang, L.; Zhu, C.; Zhou, Q.; Zhang, J.; She, M.; Liu, M. Experimental Characterization of Enhanced SNCR Process with Carbonaceous Gas Additives. *Chemosphere* **2017**, *177*, 149−156.
(10) Kuznetsov, G. V.; Syrodoy, S. V.; Kostoreva, A. A.; Kostoreva, Z. A.; Nigay, N. A. Effect of Concentration and Relative Position of Wood and Coal Particles on the Characteristics of the Mixture Ignition Process. *Fuel* **2020**, *274*, 117843.
(11) Zheng, S.; Yang, Y.; Li, X.; Liu, H.; Yan, W.; Sui, R.; Lu, Q. Temperature and Emissivity Measurements from Combustion of Pine Wood, Rice Husk and Fir Wood Using Flame Emission Spectrum. *Fuel Process. Technol.* **2020**, *204*, 106423.
(12) Kazagic, A.; Hodzic, N.; Metovic, S. Co-combustion of Low-Rank Coal with Woody Biomass and Miscanthus: An Experimental Study. *Energies* **2018**, *11*, 601.
(13) Pisa, I. Combined Primary Methods for NOx Reduction to the Pulverized Coal-Sawdust Co-combustion. *Fuel Process. Technol.* **2013**, *106*, 429−438.
(14) Zhang, L.; Duan, F.; Wu, X. NO and SO2 Removal and Pore Structure Evolution during Reburning with Calcium Magnesium Acetate Blended Peanut Shell. *J. Energy Inst.* **2020**, *93*, 614−623.
(15) Liu, X.; Chen, M.; Wei, Y. Combustion Behavior of Corncob/Bituminous Coal and Hardwood/Bituminous Coal. *Renew. Energy.* **2015**, *81*, 355−365.
(16) Niu, Y.; Tan, H.; Hui, S. e. Ash-Related Issues during Biomass Combustion: Alkali-Induced Slagging, Silicate Melt-Induced Slagging (ash fusion), Agglomeration, Corrosion, Ash Utilization, and Related Countermeasures. *Prog. Energy Combust. Sci.* **2016**, *52*, 1−61.
(17) Wu, S.; Wang, W.; Ren, C.; Yao, X.; Yao, Y.; Zhang, Q.; Li, Z. Calcination of Calcium Sulphoaluminate Cement Using Flue Gas Desulfurization Gypsum as Whole Calcium Oxide Source. *Constr. Build. Mater.* **2019**, *228*, 116676.
(18) Niu, S.; Han, K.; Lu, C. Release of Sulfur Dioxide and Nitric Oxide and Characteristic of Coal Combustion under the Effect of Calcium Based Organic Compounds. *Chem. Eng. J.* **2011**, *168*, 255−261.
(19) Daood, S. S.; Javed, M. T.; Gibbs, B. M.; Nimmo, W. NOx Control in Coal Combustion by Combining Biomass Co-firing, Oxygen Enrichment and SNCR. *Fuel* **2013**, *105*, 283−292.
(20) Shen, B.; Zhu, S.; Zhang, X.; Chi, G.; Patel, D.; Si, M.; Wu, C. Simultaneous Removal of NO and Hg0 Using Fe and Co Co-doped Mn-Ce/TiO2 Catalysts. *Fuel* **2018**, *224*, 241−249.
(21) Zhang, W.; Tang, Y.; Lu, C.; Zou, J.; Ruan, M.; Yin, Y.; Qing, M.; Song, Q. Enhancement of Catalytic Activity in NH3-SCR Reaction by Promoting Dispersibility of CuCe/TiO2-ZrO2 with Ultrasonic Treatment. *Ultrason. Sonochem.* **2021**, *72*, 105466.
(22) Cao, J.; Yao, X.; Chen, L.; Kang, K.; Fu, M.; Chen, Y. Effects of Different Introduction Methods of Ce4+ and Zr4+ on Denitration Performance and Anti-K Poisoning Performance of V2O5-WO3/TiO2 catalyst. *J. Rare Earths* **2020**, *38*, 1207−1214.
(23) Gong, P.; Xie, J.; Fang, D.; Liu, X.; He, F.; Li, F. Novel Heterogeneous Denitrification Catalyst over A Wide Temperature Range: Synergy Between CeO2, ZrO2 and TiO2. *Chem. Eng. J.* **2019**, *356*, 598−608.
(24) Yi, H.; Yang, K.; Tang, X.; Zhao, S.; Gao, F.; Xie, X.; Huang, Y.; Shi, Y.; Zhang, R. Ultrasound-assisted modification of Al 2 O 3 @ TiO 2 -Ce core-shell structure adsorbent for simultaneous desulfurization and denitrification. *J. Chem. Technol. Biotechnol.* **2020**, *95*, 2261−2271.
(25) Zhao, Y.; Wang, S.; Shen, Y.; Lu, X. Effects of Nano-TiO2 on Combustion and Desulfurization. *Energy* **2013**, *56*, 25−30.
(26) Wang, S.; Liu, L.; Yin, D. Release Characteristics of Mercury during the Combustion of Mixed coal. *J. China Coal Society* **2020**, *45*, 3921−3929.
(27) Wang, S.-Q.; Liu, M.-Z.; Sun, L.-L.; Cheng, W.-L. Study on the Mechanism of Desulfurization and Denitrification Catalyzed by TiO2 in the Combustion with Biomass and Coal. *Korean J. Chem. Eng.* **2017**, *34*, 1882−1888.
(28) Gani, A.; Naruse, I. Effect of Cellulose and Lignin Content on Pyrolysis and Combustion Characteristics for Several Types of Biomass. *Renew. Energy.* **2007**, *32*, 649−661.
(29) Oladejo, J.; Adegbite, S.; Gao, X.; Liu, H.; Wu, T. Catalytic and Non-catalytic Synergistic Effects and Their Individual Contributions to Improved Combustion Performance of Coal/Biomass Blends. *Appl. Energy.* **2018**, *211*, 334−345.
(30) Chen, H.; Liu, Z.; Chen, X.; Chen, Y.; Dong, Z.; Wang, X.; Yang, H. Comparative Pyrolysis Behaviors of Stalk, Wood and Shell Biomass: Correlation of Cellulose Crystallinity and Reaction Kinetics. *Bioresour. Technol.* **2020**, *310*, 123498.
(31) Burhenne, L.; Messmer, J.; Aicher, T.; Laborie, M.-P. The Effect of the Biomass Components Lignin, Cellulose and Hemi-

cellulose on TGA and Fixed Bed Pyrolysis. *J. Anal. Appl. Pyrolysis* **2013**, *101*, 177−184.
(32) Galina, N. R.; Romero luna, C. M.; Arce, G. L. A. F.; Ávila, I. Comparative Study on Combustion and Oxy-Fuel Combustion Environments Using Mixtures of Coal with Sugarcane Bagasse and Biomass Sorghum Bagasse by the Thermogravimetric Analysis. *J. Energy Inst.* **2019**, *92*, 741−754.

https://doi.org/10.1021/acsomega.1c04675
ACS Omega 2021, 6, 33676−33684